Current Research in Agricultural Sciences
2025 Vol. 12, No. 2, pp. 193-201
ISSN(e): 2312-6418
ISSN(p): 2313-3716
DOI: 10.18488/cras.v12i2.4599

Preparation of green-nano zinc, and study its inhibitory effect on powdery mildew disease under laboratory conditions

Shimaa Ragab Hamed[1]
Rasha El-said Abdel-Hak[2+]
Mohamed Maher Saad Saleh[3]

[1]*Microbial Biotechnology Department, Biotechnology Research Institute, National Research Centre, 33 El-Buhouth St., Dokki, Cairo 12622, Egypt.*
[1]*Email: shemo22003@yahoo.com*
[2,3]*Pomology Department, Biological and Agricultural Research Institute, National Research Centre, 33 El-Buhouth St., Dokki, Cairo 12622, Egypt.*
[2]*Email: rashaabdelhak777@gmail.com*
[3]*Email: mmsssa2000@yahoo.com*


(+ Corresponding author)

Article History
Received: 10 November 2025
Revised: 12 December 2025
Accepted: 16 December 2025
Published: 19 December 2025

Keywords
Bio-control
Biogenic ZnO
Eco-friendly nano pesticide
Green nano
Powdery mildew disease
Saccharomyces cerevisiae.

ABSTRACT

The present study focuses on the preparation of green-synthesized zinc oxide nanoparticles (ZnO NPs) using Saccharomyces cerevisiae extract and evaluates their inhibitory effect on powdery mildew disease under laboratory conditions. Powdery mildew, caused by *Erysiphe necator*, is a major fungal pathogen that reduces crop yield, leaf quality, and overall plant vigor. Conventional fungicides are widely used to control this disease; however, their repeated application raises concerns regarding environmental safety, pathogen resistance, and chemical residues in food. Consequently, there is a growing interest in developing eco-friendly alternatives that combine effectiveness with sustainability. Nanotechnology, particularly the use of biologically synthesized nanoparticles, has emerged as a promising approach to plant disease management. In this study, ZnO NPs were synthesized using an eco-friendly biological method and characterized through various techniques, including Fourier-transform infrared spectroscopy (FTIR), scanning electron microscopy (SEM), X-ray diffraction (XRD), and UV-visible spectroscopy. These methods confirmed the morphology and crystalline structure of the nanoparticles. The antifungal activity of three concentrations 50, 100, and 150 ppm was evaluated against powdery mildew leaf spot symptoms to determine their effectiveness in controlling this plant disease. Results demonstrated that ZnO NPs exhibited inhibitory activity at all tested concentrations, with effectiveness increasing proportionally to the dosage. The minimum inhibitory concentration (MIC) was determined to be 50 µg/mL, indicating strong suppression of E. necator. The study provides valuable insights into the potential application of nanotechnology in plant protection and supports the development of sustainable agricultural practices.

Contribution/Originality: This paper is distinctive because it employs *Saccharomyces cerevisiae* for the green synthesis of ZnO nanoparticles and evaluates their antifungal activity against *Erysiphe necator*, a major grapevine pathogen that is rarely studied in nanoparticle research. The study results indicate an effective concentration of 50 µg/mL, highlighting the potential as sustainable alternatives to chemical fungicides.

1. INTRODUCTION

One of the most pervasive and harmful diseases in the world is powdery mildew. A significant portion of the damage caused by this disease is attributed to *Erysiphe necator*. Numerous plant species and cultivars have leaves and

fruits that are highly vulnerable to this disease [1]. Powdery mildew can grow in a variety of humidity levels, but it is most likely to flourish in a dry climate [2].

Fruit productivity and quality could be significantly reduced due to *Erysiphe necator*'s ability to infect all green tissues, including leaves, young bunches, inflorescences, and fruits. This is because *Erysiphe necator* can lower the assimilation rate by reducing the area of green leaf tissue and affecting gas exchange in other green tissues [3, 4].

In grapevines, the initial signs are small, chlorotic dots on the upper surface of the leaf, occasionally accompanied by shiny spots or a white web on the underside. On shaded leaves, however, the symptoms are the same on both sides [2, 5].

It was once well acknowledged that several control methods, such as field sanitation and the use of appropriate fertilizers, may aid in preventing the spread of disease; nevertheless, these approaches eventually lose their ability to effectively eradicate the disease. Consequently, clever, effective, and efficient materials that are suitable for antimicrobial agents must be developed [6].

Nanotechnology may address this issue by producing nanoparticle-based pesticides that can provide an affordable and ecologically beneficial solution for managing plant diseases and crop protection [7, 8]. Moreover, soil pollution is reduced, and soil microbial communities are preserved when nanomaterials are used in agriculture to ensure the minimal use of agrochemicals [8-10].

Zinc oxide (ZnO) is a commonly used oxide due to its antimicrobial potential, demonstrated by its antifungal and antibacterial properties [11-13]. Numerous studies have shown that ZnO nanoparticles enhance antibacterial activity when doped with other metals such as chromium, silver, or gold. Additionally, it has been observed that at higher dosages, smaller nanoparticles exhibit more effective inhibition [14, 15].

This paper aims to provide information on the synthesis of ZnO nanoparticles using yeast extract and to investigate its impact on powdery mildew leaf spot disease.

2. MATERIAL AND METHODS

2.1. Synthesis of Different Nano-Particles Using Yeast Cells

The synthesis of nanoparticles (NPs) by supplementing yeast with zinc oxide (ZnO) will be used to enhance Saccharomyces cerevisiae separately. Growth media (YEPD) consisted of glucose, peptone, and yeast extract.

An incorporated strategy was employed to enrich the yeast with zinc oxide [16]. After 24 hours of incubation during the growth phase, the yeast will be inserted for integration in the second step.

2.2. Measuring the Elements Level in the Yeast Cells

A modified Demirci and Pometto [17] method was employed for sample preparation using Atomic Absorption Spectroscopy (AAS). After centrifuging the yeast sample at 10,000 rpm and 4°C for 15 minutes, the supernatant was removed. Cells were washed three times with 0.9% saline solution to remove all of the culture media adsorbed on their surfaces. A 300 mL Kjeldahl flask contained a 0.1 g dry yeast sample. The dried sample was treated with 5 mL of concentrated nitric acid and heated at 160°C until the vigorous reaction subsided. Subsequently, 2 mL of concentrated sulfuric acid was added, and heating continued while small amounts of concentrated nitric acid were added until the solution became colorless. Heating was maintained until dense sulfuric acid fumes were produced. After cooling, the contents were filtered into a 50 mL volumetric flask and diluted with distilled water to the specified volume. The sample's absorbance was measured using a Flame Atomic Absorption Spectrophotometer at 213.9 nm.

2.3. Zn Nps Characterization

2.3.1. Characterization Through Visuals

The color change in the reaction mixture from white to yellowish (ZnO NPs) was used to characterize the nanoparticle production process.

2.3.2. Ultraviolet-Visible Spectroscopy

To determine the surface plasmon resonance peaks of the biosynthesized nanoparticles, the different colloidal solutions were monitored using a UV-visible spectrophotometer (Carry 100 Ultraviolet-Visible Spectrophotometer, Agilent, USA) at a resolution of 1 nm within a wavelength range of 300 to 700 nm.

2.3.3. HRTEM

HRTEM (JEOL JEM-1200, Japan) was used to examine the size, shape, and selected area electron diffraction pattern (SAED) of the biosynthesized nanoparticles (NPs) at an operating voltage of 200 keV. Before examination by HRTEM, a drop of colloidal NPs was placed on a copper grid covered with carbon and allowed to dry in the air.

2.3.4. DLS

The particle size distribution was determined by analyzing the dynamic variations in light scattering intensity (DLS) caused by the particles' Brownian motion, using a Nano-Zeta Sizer (Malvern Instruments ZS-Nano, UK). The measurement provided several key parameters, including the zeta potential, the polydispersity index (PdI), which indicates the width of the particle size distribution, the average hydrodynamic diameter of the particles, and the peak values within the hydrodynamic diameter distribution. On the PdI scale, a value of 0 indicates a monodisperse sample, while a value of 1 indicates a highly polydisperse sample. All measurements were conducted at a scattering angle of 90°, with a temperature equilibration time of 1 minute at 25°C, and each measurement was performed in triplicate to ensure accuracy and reproducibility.

2.3.5. FTIR

Separately, the synthesized nanoparticles (NPs) were combined with spectroscopy-grade potassium bromide (KBr) powder and pressed into 1% sample pellets for Fourier-transform infrared (FTIR) analysis. The FTIR spectra were recorded using a Jasco 600 FTIR spectrophotometer (Japan) with a resolution of 4 cm^{-1} and 32 scans, covering the spectral region from 4000 to 400 cm^{-1}.

2.4. Determination of the Infection Rate and the Effectiveness of the Proposed Materials for Controlling Powdery Mildew

2.4.1. Isolation of Fungal Pathogens

Grape was used as a sample of infected plant tissues with powdery mildew, obtained from the field and sorted separately. After slicing the infected plant samples into 3 mm pieces with a sterile razor blade and sterilizing their surfaces for two minutes in a 1% hypochlorite solution, they were placed on Potato Dextrose Agar (PDA) and incubated at room temperature for five days. After isolation, each colony was transferred to a fresh plate and maintained on PDA slants.

2.4.2. Identification of Fungal Pathogens

The pathogenic fungus identified was cultivated for seven days at 28°C on Czapek-Dox medium Robinson et al. [18]. Ainsworth [19] and Ainsworth et al. [20] state that the morphological analysis of the tested fungus, using bright field microscopy (Olympus CH40), was employed to identify the promising isolated fungus.

2.5. Studying the Antimicrobial Activity for the Tested Agents

The disc diffusion method was used to identify the zone of inhibition in order to investigate the antifungal activity of the synthesized nanoparticles (NPs) that were tested [21].

The pathogenic fungal isolates were cultivated for 10 days until sporulation on potato dextrose agar (PDA) slants at 27°C. To wash the spores, a sterile 0.01% Tween 80 solution was used. Each fungal species had approximately 10^5–10^6 spores per milliliter in the final spore preparations, as observed under the microscope [22]

Testing for antifungal activity using the disc diffusion method:

The disc diffusion method was employed to assess antifungal activity, which was quantified as the percentage inhibition of mycelium growth using the following formula.

Inhibition (%) = (C - T) × 100 / C, where C and T represent the average mycelium growth (mm) of the control and treated discs, respectively. Each test was conducted three times to ensure accuracy and reproducibility.

2.5.1. Minimum Inhibitory Concentration (MIC) Determination

An agar plate dilution procedure was used to establish the MICs in accordance with the guidelines of the Clinical and Laboratory Standards Institute, as detailed in Kang et al. [23].

3. RESULTS

3.1. Zinc Oxide Nanoparticles: Synthesis and Characterization

As illustrated in Figure 1a, ZnO nanoparticles (NPs) powder exhibited a fluffy appearance and a white to yellowish tint. Using UV-visible spectroscopic absorbance analysis, it was observed that the biosynthesized colloidal ZnO NPs remained stable for up to five months when stored at 4°C. The spectra of ZnO nanoparticles are characterized by a local absorption peak at 300–325 nm and show significant absorption in the ultraviolet (UV) region, extending well into the UV spectrum (Figure 1b).

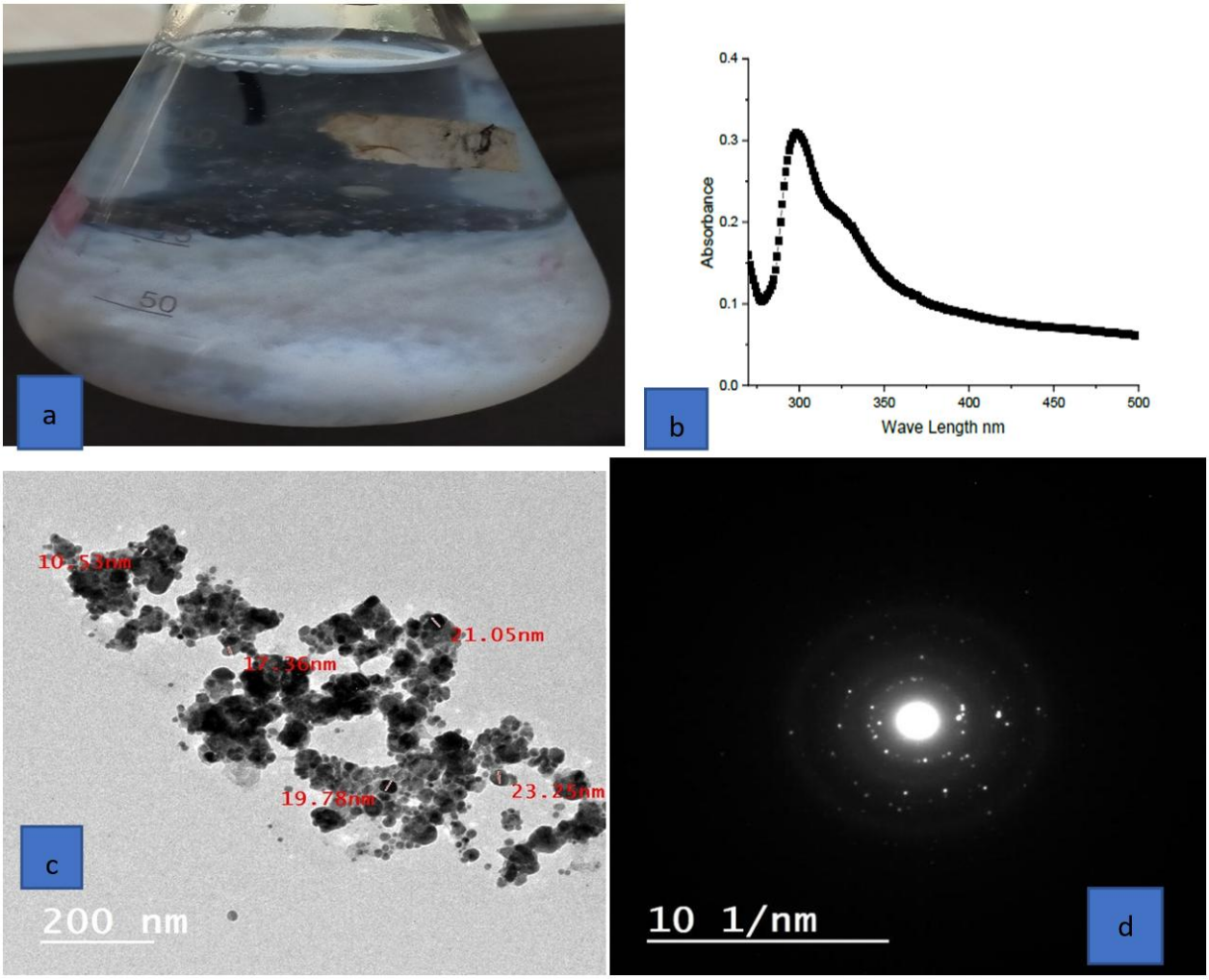

Figure 1. Characterization of ZnO NPs. (a) Bio-synthesized ZnO NPs. (b) UV image of ZnO NPs synthesized by green technology. (c, d) HRTEM micrograph image and SAED pattern of ZnO NPs, respectively.

The HRTEM method was used to examine the NPs' size, shape, and crystallinity. ZnO NP HRTEM micrographs revealed comparatively tiny spherical particles (10–23 nm) that were coagulated in sizable clusters (Figure 1c). By examining the selected area electron diffraction (SAED) pattern, which revealed fine patches in the ring pattern (Figure 1d), the polycrystalline structure of the tested ZnO nanoparticles was verified.

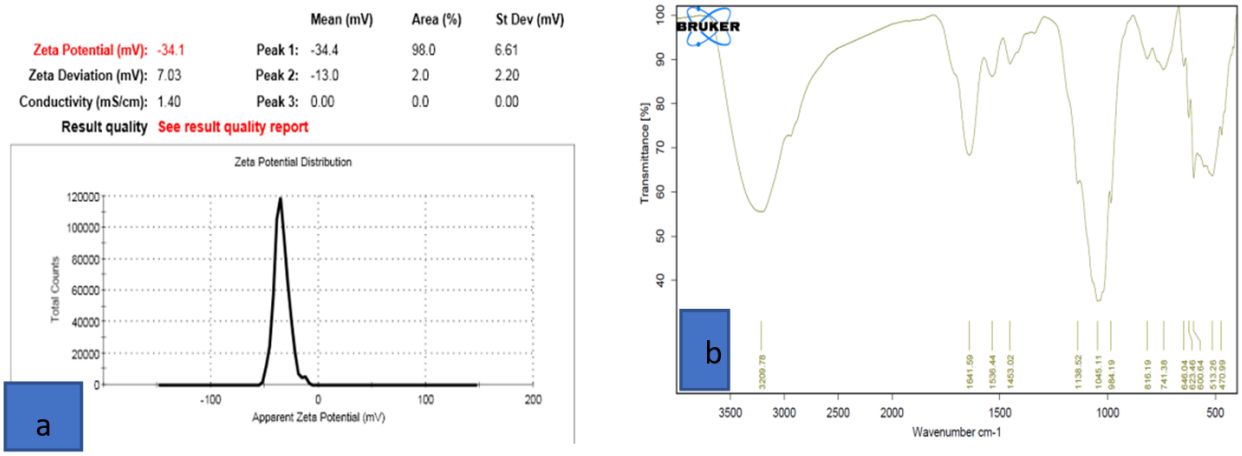

Figure 2. (a) DLS of ZnO NPs showing the size distribution by number. (b) FTIR spectra of ZnO NPs.

Table 1. DLS of the tested ZnO NPs.

Parameter	Tested ZnO NPs		
	Peak 1	Peak 2	Peak 3
Area %	98.0	2.0	0.0
PdI	6.61	2.20	0.0
Zeta potential (mv)	-34.4	-13.0	0.0

Dynamic light scattering (DLS) of the tested ZnO nanoparticles (NPs) showed three peaks with area percentages of 98.0%, 2.0%, and 0.0%, respectively, as shown in Figure 2a. Additionally, DLS indicated the polydispersity index (PdI) values of 6.61, 2.20, and 0.0, while the zeta potential measurements were -34.4 mV, -13.0 mV, and 0.0 mV, respectively (Table 1).

Based on the peak value in the infrared spectrum, FTIR spectroscopy is used to determine the functional groups of the biomolecules encasing the NPs. Figure 2b displays the ZnO NPs' FTIR spectra. These nanoparticles were capped with a protein found in yeast cells, according to the ZnO NPs spectra, which displayed absorption bands at 3209 cm^{-1}, 1641 cm^{-1}, 1536 cm^{-1}, 1453 cm^{-1}, 1138 cm^{-1}, and 1045 cm^{-1}. The peak, which was assigned to amide A's ν(N–H) and overlapped with ν(O–H), appeared at an average wave number of 3209 cm^{-1}. Additionally, the bending vibrations of the protein's amide I and amide II bands correlated with the band at 1641 cm^{-1}. Furthermore, at 1045 cm^{-1}, a band indicative of C–C–O emerged [24].

3.2. Identification of Fungal Pathogens

The morphological features of the fungal pathogen are as follows (Figure 3): After a gradual growth period, the colonies on Czapek's agar reached a diameter of 3 to 4 cm. The mycelium is amphigenous, generally scattered, and nearly permanent on the fruits. It features lobed or multilobed, single or paired appressoria, elliptic, solitary conidia devoid of fibrosin bodies. The conidiophore's foot cell experienced one or two twists. Four to six spores are observed in cleistothecia, which contain four to eight asci. The apex is not expanded, circinate loosely or tightly, and is rigid, brown throughout at least the basal part. Appendages, numbering 10-30, are equatorial, measuring 1-6 times the diameter. We verified that the fungal infection was caused by Erysiphe necator through both microscopic and macroscopic studies.

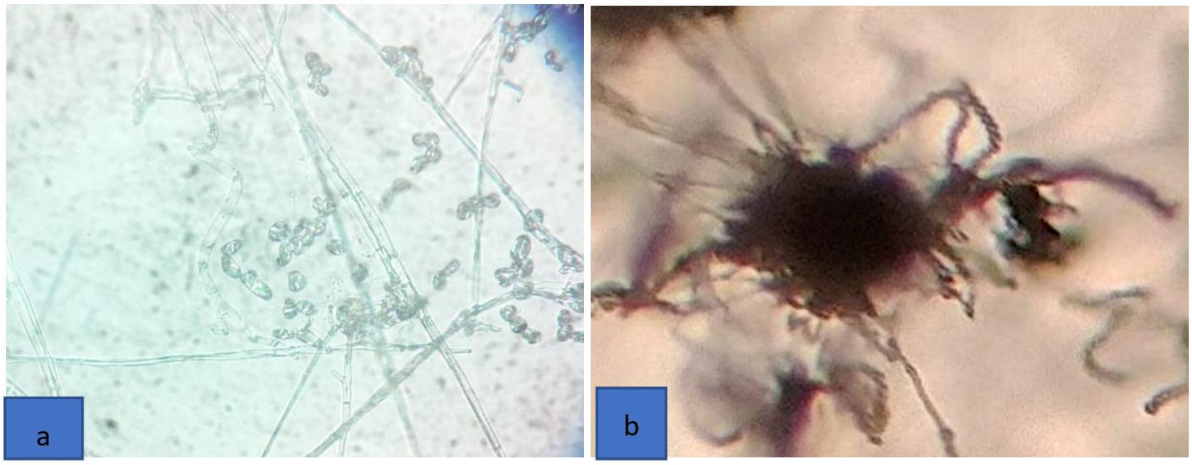

Figure 3. Micro-photographic images of powdery mildew *Erysiphe necator*: (a) Prolonged mycelia of fungi, (b) Fungal cleistothecia.

3.3. Antifungal Activity and Minimum Inhibitory Concentration (MIC) of ZnO NPs

It is well known that ZnO nanoparticles (NPs) are potential antimicrobial agents [25, 26]. The antifungal activity of ZnO NPs against plant pathogenic fungi, specifically *Erysiphe necator*, is reported here for the first time in this study. The inhibitory activity against the plant pathogen was observed at all tested concentrations, starting from the lowest one (50 µg/mL) of ZnO NPs. The minimum inhibitory concentration (MIC) of the tested ZnO NPs was found to be 150 µg/mL, with the lowest MIC observed for *Erysiphe necator*.

4. DISCUSSION

The distinctive surface plasmon resonance (SPR) of ZnO nanoparticles (NPs) contributes to their fluffy appearance and white to yellowish tint. The SPR absorbance of ZnO NPs was observed at 300-325 nm, representing the most significant absorption band identified through UV-visible spectroscopy. The absorption peaks of ZnO NPs, which range from 358 to 375 nm, are consistent with findings reported by other researchers [27, 28]. The nanoparticles were uniformly sized and spherical in shape. They appear to be evenly spaced and tend to form clusters. Various shapes of ZnO NPs, including spherical, pyramidal, rectangular, pentagonal, hexagonal, and irregular forms, have been documented in scientific literature [29, 30]. ZnO NPs were found to have a low zeta potential while remaining stable for approximately five months when stored at 4°C. This stability is primarily due to steric repulsion between the layers of biomolecules, as van der Waals forces are too weak at those distances to cause the particles to aggregate [31].

The FTIR data clearly demonstrated that the formation and stability of ZnO nanoparticles (NPs) were facilitated by fungal biomolecules, specifically proteins. It is well established that interactions between nanoparticles and proteins occur through electrostatic attraction involving free amino groups or cysteine residues in proteins, as well as negatively charged carboxylate groups in enzyme proteins [24]. Many researchers have reported that ZnO NPs were covered by protein molecules generated by microorganisms, which is consistent with these findings [31].

Because pathogenic fungi are resistant to traditional treatments, there is a greater need to find innovative and affordable biocontrol agents. Since ZnO NPs have been shown to have excellent antibacterial activity against a variety of bacteria, viruses, fungi, and protozoa, it is widely recognized that they have the potential to be an antimicrobial agent [32-34]. The ZnO nanoparticles (NPs) under examination have a minimum inhibitory concentration (MIC) ranging from 50 to 150 µg/mL. For ZnO NPs, four established potential antibacterial mechanisms are recognized: (1) ZnO NPs lose their permeability feature when they adhere to the microorganism's surface membrane; (2) they penetrate the cell wall and disrupt biomolecules, leading to intracellular damage; (3) they induce cellular toxicity by

producing reactive oxygen species (ROS), which trigger oxidative stress within the cell; and (4) they interfere with the cells' signal transduction pathways [35, 36].

Funding: This study received no specific financial support.
Institutional Review Board Statement: Not applicable.
Transparency: The authors state that the manuscript is honest, truthful, and transparent, that no key aspects of the investigation have been omitted, and that any differences from the study as planned have been clarified. This study followed all writing ethics.
Competing Interests: The authors declare that they have no competing interests.
Authors' Contributions: All authors contributed equally to the conception and design of the study. All authors have read and agreed to the published version of the manuscript.

REFERENCES

[1] R. C. Pearson and D. M. Gadoury, *Grape powdery mildew. In J. Kumar & H. S. Chaube (Eds.), Plant diseases of international importance: Diseases of fruit crops*. Englewood Cliffs, NJ: Prentice Hall, 1992.

[2] M. E. Sadek, Y. M. Shabana, K. Sayed-Ahmed, and A. H. Abou Tabl, "Antifungal activities of sulfur and copper nanoparticles against cucumber postharvest diseases caused by Botrytis cinerea and Sclerotinia sclerotiorum," *Journal of Fungi*, vol. 8, no. 4, p. 412, 2022. https://doi.org/10.3390/jof8040412

[3] U. Mueen *et al.*, "Powdery mildew: A disease of grapes and the fungicides' mode of action: A review," *Biosight*, vol. 3, no. 2, pp. 38-52, 2022.

[4] M. Moriondo, S. Orlandini, A. Giuntoli, and M. Bindi, "The effect of downy and powdery mildew on grapevine (Vitis vinifera L.) leaf gas exchange," *Journal of Phytopathology*, vol. 153, no. 6, pp. 350-357, 2005. https://doi.org/10.1111/j.1439-0434.2005.00984.x

[5] R. C. Pearson and A. C. Goheen, *Compendium of grape diseases*. St. Paul, MN, USA: APS Press, 1988.

[6] P. Fincheira, G. Tortella, A. B. Seabra, A. Quiroz, M. C. Diez, and O. Rubilar, "Nanotechnology advances for sustainable agriculture: Current knowledge and prospects in plant growth modulation and nutrition," *Planta*, vol. 254, no. 4, p. 66, 2021. https://doi.org/10.1007/s00425-021-03714-0

[7] D. G. Panpatte, Y. K. Jhala, H. N. Shelat, and R. V. Vyas, "Nanoparticles: The next generation technology for sustainable agriculture. In Microbial inoculants in sustainable agricultural productivity: Functional applications," vol. 2. New Delhi: Springer India, 2016, pp. 289-300.

[8] I. Ul Haq and S. Ijaz, *Use of metallic nanoparticles and nanoformulations as nanofungicides for sustainable disease management in plants. In Prasad, R., Kumar, V., Kumar, M., Choudhary, D. (Eds.), Nanobiotechnology in Bioformulations. Nanotechnology in the Life Sciences*. Cham: Springer International Publishing, 2019.

[9] Y. Shang, M. K. Hasan, G. J. Ahammed, M. Li, H. Yin, and J. Zhou, "Applications of nanotechnology in plant growth and crop protection: A review," *Molecules*, vol. 24, no. 14, p. 2558, 2019. https://doi.org/10.3390/molecules24142558

[10] H. Bahrulolum *et al.*, "Green synthesis of metal nanoparticles using microorganisms and their application in the agrifood sector," *Journal of Nanobiotechnology*, vol. 19, no. 1, p. 86, 2021. https://doi.org/10.1186/s12951-021-00834-3

[11] P. J. P. Espitia, N. D. F. F. Soares, J. S. D. R. Coimbra, N. J. D. Andrade, R. S. Cruz, and E. A. A. Medeiros, "Zinc oxide nanoparticles: Synthesis, antimicrobial activity and food packaging applications," *Food and Bioprocess Technology*, vol. 5, pp. 1447–1464, 2012. https://doi.org/10.1007/s11947-012-0797-6

[12] P. Jamdagni, P. Khatri, and J. S. Rana, "Green synthesis of zinc oxide nanoparticles using flower extract of Nyctanthes arbor-tristis and their antifungal activity," *Journal of King Saud University – Science*, vol. 30, no. 2, pp. 168–175, 2018. https://doi.org/10.1016/j.jksus.2016.10.002

[13] M. A. Ansari, H. M. Khan, A. A. Khan, A. Sultan, and A. Azam, "Synthesis and characterization of the antibacterial potential of ZnO nanoparticles against extended-spectrum β-lactamases-producing Escherichia coli and Klebsiella pneumoniae isolated from a tertiary care hospital of North India," *Applied Microbiology and Biotechnology*, vol. 94, no. 2, pp. 467-477, 2012. https://doi.org/10.1007/s00253-011-3733-1

[14] A. H. Shah, E. Manikandan, M. B. Ahamed, D. A. Mir, and S. A. Mir, "Antibacterial and Blue shift investigations in sol–gel synthesized CrxZn1− xO Nanostructures," *Journal of Luminescence*, vol. 145, pp. 944-950, 2014. https://doi.org/10.1016/j.jlumin.2013.09.023

[15] A. B. P. Jiménez, C. A. H. Aguilar, J. M. V. Ramos, and P. Thangarasu, "Synergistic antibacterial activity of nanohybrid materials ZnO–Ag and ZnO–Au: Synthesis, characterization, and comparative analysis of undoped and doped ZnO nanoparticles," *Australian Journal of Chemistry*, vol. 68, no. 2, pp. 288-297, 2015. https://doi.org/10.1071/CH14123

[16] S. R. Hamed, R. S. Abdel-Hak, M. M. S. Saleh, and A.-R. M. A. Merwad, "Impact of active fresh yeast enriched with Zn on yield and fruit properties of flame seedless grapes," *Egyptian Journal of Chemistry*, vol. 66, no. 2, pp. 435-448, 2023. https://doi.org/10.21608/ejchem.2022.135243.5947

[17] A. Demirci and A. L. Pometto, "Production of organically bound selenium yeast by continuous fermentation," *Journal of Agricultural and Food Chemistry*, vol. 47, no. 6, pp. 2491-2495, 1999. https://doi.org/10.1021/jf981198y

[18] M. Robinson, J. Riov, and A. Sharon, "Indole-3-acetic acid biosynthesis in colletotrichum gloeosporioides f. sp. aeschynomene," *Applied and Environmental Microbiology*, vol. 64, no. 12, pp. 5030-5032, 1998. https://doi.org/10.1128/AEM.64.12.5030-5032.1998

[19] G. C. Ainsworth, *Ainsworth and Bisby's dictionary of the Fungi*, 6th ed. UK: Commonwealth Agricultural Bureau, 1971.

[20] G. C. Ainsworth, G. R. Bisby, and P. M. Kirk, *Ainsworth and Bisby's dictionary of the Fungi*. England: CABI, 2008.

[21] N. S. Alzoreky and K. Nakahara, "Antibacterial activity of extracts from some edible plants commonly consumed in Asia," *International Journal of Food Microbiology*, vol. 80, no. 3, pp. 223-230, 2003. https://doi.org/10.1016/S0168-1605(02)00169-1

[22] M. Abril, K. J. Curry, B. J. Smith, and D. E. Wedge, "Improved microassays used to test natural product-based and conventional fungicides on plant pathogenic fungi," *Plant Disease*, vol. 92, no. 1, pp. 106-112, 2008. https://doi.org/10.1094/PDIS-92-1-0106

[23] C.-G. Kang, D.-S. Hah, C.-H. Kim, Y.-H. Kim, E. Kim, and J.-S. Kim, "Evaluation of antimicrobial activity of the methanol extracts from 8 traditional medicinal plants," *Toxicological Research*, vol. 27, no. 1, pp. 31-36, 2011. https://doi.org/10.5487/TR.2011.27.1.031

[24] A. Gole *et al.*, "Pepsin− gold colloid conjugates: Preparation, characterization, and enzymatic activity," *Langmuir*, vol. 17, no. 5, pp. 1674-1679, 2001. https://doi.org/10.1021/la001164w

[25] M. A. Huq *et al.*, "Bioactive ZnO nanoparticles: Biosynthesis, characterization and potential antimicrobial applications," *Pharmaceutics*, vol. 15, no. 11, p. 2634, 2023. https://doi.org/10.3390/pharmaceutics15112634

[26] M. Kaushik *et al.*, "Investigations on the antimicrobial activity and wound healing potential of ZnO nanoparticles," *Applied Surface Science*, vol. 479, pp. 1169-1177, 2019. https://doi.org/10.1016/j.apsusc.2019.02.189

[27] H. Hameed *et al.*, "Green synthesis of zinc oxide (ZnO) nanoparticles from green algae and their assessment in various biological applications," *Micromachines*, vol. 14, no. 5, p. 928, 2023. https://doi.org/10.3390/mi14050928

[28] P. Manimegalai *et al.*, "Green synthesis of zinc oxide (ZnO) nanoparticles using aqueous leaf extract of Hardwickia binata: Their characterizations and biological applications," *Biomass Conversion and Biorefinery*, vol. 14, no. 11, pp. 12559-12574, 2024. https://doi.org/10.1007/s13399-023-04279-6

[29] T. Gur, I. Meydan, H. Seckin, M. Bekmezci, and F. Sen, "Green synthesis, characterization and bioactivity of biogenic zinc oxide nanoparticles," *Environmental Research*, vol. 204, p. 111897, 2022. https://doi.org/10.1016/j.envres.2021.111897

[30] S. A. Rasha, R. H. Shimaa, M. M. S. Saleh, and M. A. Merwad, "The beneficial effect of yeast enriched with nano zinc particles on mineral status of grape seedlings," *International Journal of Research and Innovation in Applied Science*, vol. 8, pp. 203-211, 2023.

[31] L. M. Liz-Marzan *et al.*, *Core–shell nanoparticles and assemblies thereof. In H. S. Nalwa (Ed.), Handbook of Surfaces and Interfaces of Materials*. USA: Academic Press, 2001.

[32] G. R. Navale, M. Thripuranthaka, J. L. Dattatray, and S. S. Sandip, "Antimicrobial activity of ZnO nanoparticles against pathogenic bacteria and fungi," *JSM Nanotechnology & Nanomedicine*, vol. 3, p. 1033, 2015.

[33] H. Mohd Yusof, N. A. Abdul Rahman, R. Mohamad, U. H. Zaidan, and A. A. Samsudin, "Biosynthesis of zinc oxide nanoparticles by cell-biomass and supernatant of Lactobacillus plantarum TA4 and its antibacterial and biocompatibility properties," *Scientific Reports*, vol. 10, no. 1, p. 19996, 2020. https://doi.org/10.1038/s41598-020-76402-w

[34] L. Motelica *et al.*, "Biodegradable alginate films with ZnO nanoparticles and citronella essential oil—A novel antimicrobial structure," *Pharmaceutics*, vol. 13, no. 7, p. 1020, 2021. https://doi.org/10.3390/pharmaceutics13071020

[35] Y. Xie, Y. He, P. L. Irwin, T. Jin, and X. Shi, "Antibacterial activity and mechanism of action of zinc oxide nanoparticles against Campylobacter jejuni," *Applied and Environmental Microbiology*, vol. 77, no. 7, pp. 2325-2331, 2011. https://doi.org/10.1128/AEM.02149-10

[36] W. Gemechis and C. Bayissa, " The role of biosynthesized metallic and metal oxide nanoparticles in combating anti-microbial drug resilient pathogens," *Journal of Biomaterials and Nanobiotechnology*, vol. 14, no. 1, pp. 1-22, 2023. https://doi.org/10.4236/jbnb.2023.141001